

# Stability of position control of traveling waves in reaction-diffusion systems

Jakob Löber\*

*Institut für Theoretische Physik, EW 7-1, Hardenbergstraße 36,  
Technische Universität Berlin, 10623 Berlin, Germany*

We consider the stability of position control of traveling waves in reaction-diffusion system as proposed in [J. Löber, H. Engel, [arXiv:1304.2327](#)]. Instead of analyzing the controlled reaction-diffusion system, stability is studied on the reduced level of the equation of motion for the position over time of perturbed traveling waves. We find an interval of perturbations of initial conditions for which position control is stable. This interval can be interpreted as a localized region where traveling waves are susceptible to perturbations. For stationary solutions of reaction-diffusion systems with reflection symmetry, this region does not exist. Analytical results are in qualitative agreement with numerical simulations of the controlled Schlögl model.

PACS numbers: 82.40.Ck, 02.30.Yy, 82.40.Bj

## I. INTRODUCTION

Beside the well-known Turing patterns, reaction-diffusion systems (RDS) possess a rich variety of traveling waves including propagating fronts, solitary excitation pulses and periodic pulse trains in one-dimensional media, target patterns and spiral waves and wave segments in two respectively scroll waves in three spatial dimensions.

Quite different approaches have been developed for purposeful manipulation of wave dynamics as the application of feedback-mediated control loops with and without delays, external spatiotemporal forcing or imposing heterogeneities and geometric constraints on the medium [1–4]. For example, unstable patterns can be stabilized by global feedback control, as was shown in experiments with the light-sensitive Belousov-Zhabotinsky (BZ) reaction [5, 6]. Varying the excitability of the light-sensitive BZ medium by changing the globally applied light intensity, forces a spiral wave tip to describe a wide range of hypocycloidal and epicycloidal trajectories [7–9]. BZ spirals were subjected to a feedback based on the wave activity measured in a certain detector point, along a given line detector, or in a given spatial domain. It was demonstrated that the spiral tip behavior can be controlled by the feedback strength and the delay time in the feedback loop, but also by the geometrical arrangement of the detectors as well as by the size and the shape of the spatial domain from which the feedback signal is determined [10, 11]. Two feedback loops were used to stabilize unstable wave segments and to guide their propagation direction [12].

Dragging of a traveling chemical pulse [13] on an addressable catalyst surface [14–16] was accomplished by a moving, localized temperature heterogeneity. Dragging of fronts in chemical and phase transitions models as well as targeted transfer of nonlinear Schrödinger pulses by moving heterogeneities was studied in [17–19].

In our recent work [20], we proposed an efficient control method realized by a localized spatio-temporal forcing  $\mathbf{f}(x, t)$  which allows to control the position over time of a traveling wave according to a protocol of movement  $\phi(t)$  while simultaneously preserving the wave profile  $\mathbf{U}_c$  of the uncontrolled wave.

The solution for the control function is found by solving a perturbatively obtained integral equation for the control, which is usually seen as an ordinary differential equation (ODE) for the position over time  $\phi(t)$  of the wave under the perturbation  $\mathbf{f}$ . This ODE is also known as an equation of motion for traveling waves and provides a reduction of a solitary moving wave to its particle properties.

To formulate the control function, only knowledge of the uncontrolled wave profile  $\mathbf{U}_c$  and its velocity  $c$  are necessary. In particular, no knowledge of the underlying reaction kinetics is required. For a variety of reaction-diffusion models we demonstrated the ability of the control method to enforce e.g. accelerating, decelerating and oscillating movements in on spatial dimension. Furthermore, for these examples we showed that the proposed solution for the control function  $\mathbf{f}(x, t)$  is close to a numerically obtained optimal control solution.

However, we did not clarify in detail the mechanism leading to a successful position control. Furthermore, one would like to narrow down the conditions under which one can expect the control method work.

Here, we partially answer these questions, not on the level of the controlled reaction-diffusion system, but on the level of the equation of motion. We will consider stability against perturbations of the initial conditions. Initially, the localized control  $\mathbf{f}(x, t)$  is not applied exactly at the position of the traveling wave, but at a distance  $\Delta X_0$  away from it. If  $\Delta X_0$  grows unboundedly in time, position control is unstable. It will turn out to be necessary to do a nonlinear stability analysis to get a useful answer. We give a short introduction about what we actually mean by nonlinear stability in appendix A.

We will find that position control is stable against perturbations of initial conditions which lie in a certain interval. It is well known that due to the localization of traveling

---

\* [jakob@physik.tu-berlin.de](mailto:jakob@physik.tu-berlin.de)

waves, a perturbation has only an effect if it is applied near to the position of the wave, and has no effect if it is applied elsewhere. The region of stable initial conditions can be interpreted as such a “region of sensitivity” near to the wave’s position.

The paper is organized as follows. In Sec. II, we state the equations of motion of traveling waves. Sec. III considers how the equation of motion is utilized to obtain a control function for position control. Subsequently we describe the approach to prove the stability of the proposed solution for the control function (Sec. IV). We consider single component (Sec. V) and multicomponent (Sec. VI) models. Stationary solutions behave differently under position control and are considered in Sec. VII. Sec. VIII comprises a summary and conclusions.

## II. EQUATION OF MOTION FOR TRAVELING WAVES

We consider a perturbed reaction-diffusion system for the vector of  $n$  components  $\mathbf{u} = (u_1, \dots, u_n)^T$  in a one-dimensional infinitely extended medium,

$$\partial_t \mathbf{u} = D \partial_x^2 \mathbf{u} + \mathbf{R}(\mathbf{u}) + \epsilon \mathcal{G}(\mathbf{u}) \mathbf{f}(x, t), \quad (1)$$

Here,  $D$  is a diagonal matrix of constant diffusion coefficients,  $\mathbf{f}$  is a spatiotemporal perturbation coupled to the system by a (possibly  $\mathbf{u}$ -dependent) square matrix  $\mathcal{G}$ , and  $\mathbf{R}$  is a typically nonlinear reaction function. Traveling wave solution  $\mathbf{U}_c(\xi)$  of the unperturbed RDS, Eq. (1) with  $\epsilon = 0$ , are stationary solutions in a comoving frame of reference  $\xi = x - ct$

$$0 = D \partial_\xi^2 \mathbf{U}_c(\xi) + c \partial_\xi \mathbf{U}_c(\xi) + \mathbf{R}(\mathbf{U}_c(\xi)), \quad (2)$$

where  $c$  denotes the velocity of the traveling wave. Stationary solutions with  $c = 0$  are also considered as traveling waves.

The ordinary differential equation (ODE) for the wave profile, Eq. (2), can exhibit one or more homogeneous steady states. Typically, for  $\xi \rightarrow \pm\infty$ , the wave profile approaches either two different steady states or the same steady states. This can be used to classify traveling wave profiles. Front profiles connect different steady states for  $\xi \rightarrow \pm\infty$  and are found to be heteroclinic orbits of Eq. (2), while pulse solutions join the same steady state and are found to be homoclinic orbits. Pulse profiles are naturally localized and usually every component exhibits one or several extrema. Fronts are not localized but typically exhibit a narrow region where the transition from one to the other steady state occurs. Therefore, all traveling wave solutions are localized in the sense that the derivatives of any order  $n \geq 1$  of the wave profile  $\mathbf{U}_c(\xi)$  with respect to the traveling wave coordinate  $\xi$  decays to zero,

$$\lim_{\xi \rightarrow \pm\infty} \partial_\xi^n \mathbf{U}_c(\xi) = 0. \quad (3)$$

The linear stability of the traveling wave is determined by the eigenvalues  $\lambda$  of the linearization operator

$$\mathcal{L} = D \partial_\xi^2 + c \partial_\xi + \mathcal{D}\mathbf{R}(\mathbf{U}_c(\xi)) \quad (4)$$

where  $\mathcal{D}\mathbf{R}(\mathbf{U}_c(\xi))$  is the Jacobi matrix of the reaction function  $\mathbf{R}$  evaluated at the traveling wave solution  $\mathbf{U}_c$ . We assume that the traveling wave is stable such that the eigenvalue with largest real part is  $\lambda_0 = 0$  [21]. The corresponding eigenfunction is found to be the so-called Goldstone mode  $\mathbf{W}(\xi) = \partial_\xi \mathbf{U}_c(\xi)$ . Furthermore, we presume that a spectral gap separates the zero eigenvalue from the next eigenvalue  $\lambda_1$  of  $\mathcal{L}$ . That means that not only  $\Re(\lambda_1) < \lambda_0 = 0$  but the stronger assumption  $\Re(\lambda_1) < d < \lambda_0 = 0$  must hold. Here,  $d$  is an arbitrary negative real number and  $|d|$  measures the width of the spectral gap while  $\Re$  indicates the real part of a complex number. This assumption also implies that the zero eigenvalue is not degenerate and there is no other eigenvalue with zero part.

By means of a singular perturbation analysis in the small parameter  $\epsilon$ , an equation of motion for the position over time  $\phi(t)$  of a perturbed traveling wave is obtained as [22–28]

$$\dot{\phi}(t) = c - \frac{\epsilon}{K_c} \int_{-\infty}^{\infty} dx \mathbf{W}^{\dagger T}(x) \mathcal{G}(\mathbf{U}_c(x)) \mathbf{f}(x + \phi(t), t), \quad (5)$$

with constant

$$K_c = \int_{-\infty}^{\infty} dx \mathbf{W}^{\dagger T}(x) \mathbf{U}'_c(x) \quad (6)$$

and initial condition

$$\phi(t_0) = \phi_0. \quad (7)$$

The function  $\mathbf{W}^\dagger(x)$  is known as the adjoint Goldstone mode or response function. It is the eigenfunction to eigenvalue 0 of the adjoint operator  $\mathcal{L}^\dagger$  of  $\mathcal{L}$  with respect to the standard inner product in function space,

$$\mathcal{L}^\dagger \mathbf{W}^\dagger = 0. \quad (8)$$

The operator  $\mathcal{L}^\dagger$  can be obtained by partial integration and is given as

$$\mathcal{L}^\dagger = D \partial_\xi^2 - c \partial_\xi + \mathcal{D}\mathbf{R}(\mathbf{U}_c(\xi))^T. \quad (9)$$

See [28] for details of the derivation of Eq. (5).

Approaches related to the equation of motion (5) are the direct soliton perturbation theory [29, 30] developed for conservative systems supporting traveling waves as e.g. the Korteweg-de Vries equation and phase reduction methods for limit cycle solutions to dynamical systems [31].

The equation of motion Eq. (5) can be seen as a reduction of a field equation exhibiting traveling localized (soliton-like) structures to the properties of a point particle. The field equations are dissipative and result in equations of motion resembling the equations of motion of classical mechanics for an overdamped (first order time derivative for the position over time  $\dot{\phi}(t)$ ) and constantly driven (through the  $c$ -term) particle moving in a potential (the integral term depending on the position  $\phi$ ). Interestingly, reduction of conservative soliton equations as e.g. the nonlinear Schrödinger equation to particle properties often yield equations for the position over time which are not overdamped [32], though damping terms can arise through perturbations.

The mathematical derivation of the equation of motion does actually not identify a particular point of the wave profile which must be used as the position of the wave. Therefore, we define a distinguishing point of the wave profile as its position. For pulse solutions, we define an extremum of a certain component as the position of the traveling wave. For front solutions, we define it to be a characteristic point in the transition region as e.g. the point of steepest slope.

Similar to the profile of traveling waves, also response functions  $\mathbf{W}^\dagger$  are usually localized close to the position of the traveling wave. According to the equation of motion Eq. (5), a perturbation  $\mathbf{f}$  affects the position of traveling waves only if both  $\mathbf{W}^\dagger$  and  $\mathbf{f}$  are significantly different from zero at the same position. Far away from the position of a traveling wave, perturbations do not affect the wave. However, it is well known that in many RDS an overcritical perturbation of a homogeneous steady state can excite new waves. Naturally, this generation of new waves cannot be accounted for by the equation of motion. Speaking in the particle picture, the equation of motion describes the effect of perturbations onto the particle's position and velocity, but does not account for the generation of particles.

### III. POSITION CONTROL OF TRAVELING WAVES

Usually the equation of motion Eq. (5) is seen as an ODE for the position over time  $\phi(t)$ . Turning the problem upside down, we view Eq. (5) as an integral equation for the control function  $\mathbf{f}$  with an arbitrary but given *protocol of movement*  $\phi(t)$ . Without exception, we set  $\epsilon = 1$  and expect Eq. (5) to be accurate only if the perturbation  $\mathbf{f}$  is sufficiently small in amplitude. We assume that the wave moves unperturbed with velocity  $c$  until the time  $t = t_0$ , upon which the control is switched on. A general solution for the control function for an arbitrary protocol of movement  $\phi(t)$  is

$$\mathbf{f}(x, t) = \left(c - \dot{\phi}(t)\right) \frac{K_c}{G_c} \mathcal{G}^{-1}(\mathbf{U}_c(x - \phi(t))) \mathbf{h}(x - \phi(t)) \quad (10)$$

with constant

$$G_c = \int_{-\infty}^{\infty} dx \mathbf{W}^{\dagger T}(x) \mathbf{h}(x). \quad (11)$$

This control function is composed of a time-dependent amplitude  $\left(c - \dot{\phi}(t)\right) \frac{K_c}{G_c}$  and a space dependent function  $\mathbf{k}(x) = \mathcal{G}^{-1}(\mathbf{U}_c(x)) \mathbf{h}(x)$ . The spatial term involves the matrix inverse of the coupling matrix  $\mathcal{G}$  and an arbitrary vectorial function  $\mathbf{h}(x)$ . It is co-moving with the controlled wave because  $\mathbf{k}$  is evaluated at the argument  $x - \phi(t)$ . A control proportional to the Goldstone mode,  $\mathbf{f}(x, t) \sim \partial_x \mathbf{U}_c(x)$ , only shifts the traveling wave [20]. Therefore we choose

$$\mathbf{h}(x) = \mathbf{U}'_c(x) \quad (12)$$

and the full solution for the control function reads

$$\mathbf{f}(x, t) = \left(c - \dot{\phi}(t)\right) \mathcal{G}^{-1}(\mathbf{U}_c(x - \phi(t))) \mathbf{U}'_c(x - \phi(t)). \quad (13)$$

An additional advantage of this choice is, that  $K_c = G_c$  and any reference to the (usually unknown) response function  $\mathbf{W}^{\dagger T}$  cancels out. The expected effect of such a control is to shift the traveling wave solution  $\mathbf{U}_c$  according to the chosen protocol of movement such that the solution to the controlled RDS (1) with control  $\mathbf{f}$  given by Eq. (13) is approximately

$$\mathbf{u}(x, t) \approx \mathbf{U}_c(x - \phi(t)). \quad (14)$$

In [20] we showed by examples that this expectation is correct and that the control function (13) works for a large variety of RDS supporting traveling wave solutions and many protocols.

### IV. STABILITY OF POSITION CONTROL - GENERAL APPROACH

Position control of a traveling wave is successful if the wave's position follows the protocol closely and, furthermore, the wave profile is only slightly deformed. In other words, the solution  $\mathbf{u}(x, t)$  of the RDS Eq. (1) under the action of the control function  $\mathbf{f}(x, t)$ , Eq. (13), is always close, in some sense, to the traveling wave solution shifted according to the protocol  $\phi(t)$ ,

$$\mathbf{u}(x, t) \approx \mathbf{U}_c(x - \phi(t)). \quad (15)$$

To prove that this is indeed the case is certainly a difficult task and can, if at all, only be done for the simplest reaction-diffusion models. Here we follow a much simpler approach and consider the stability of position control on the level of the equation of motion Eq. (5). We distinguish between the intended position of the traveling wave given by the protocol  $X(t)$  and the true wave position

over time  $\phi(t)$ . The protocol  $X(t)$  is chosen by an external agent who is able to control the system by applying the control function

$$\mathbf{f}(x, t) = \left(c - \dot{X}(t)\right) \mathcal{G}^{-1}(\mathbf{U}_c(x - X(t))) \mathbf{U}'_c(x - X(t)), \quad (16)$$

while the true position over time is governed by the equation of motion with  $\mathbf{f}$  given by Eq. (16)

$$\begin{aligned} \dot{\phi}(t) &= c - \frac{1}{K_c} \left(c - \dot{X}(t)\right) \int_{-\infty}^{\infty} dx \mathbf{W}^{\dagger T}(x) \mathcal{G}(\mathbf{U}_c(x)) \\ \mathcal{G}^{-1}(\mathbf{U}_c(x + \phi(t) - X(t))) \mathbf{U}'_c(x + \phi(t) - X(t)). \end{aligned} \quad (17)$$

We assume that the wave moves unperturbed with velocity  $c$ ,  $\dot{\phi}(t) = c$ , for all times  $t < t_0$ . The protocol velocity  $\dot{X}(t)$  is assumed to be smooth, which implies that the protocol velocity must equal the velocity  $c$  at time  $t = t_0$ ,  $\dot{X}(t_0) = c$ . Nevertheless, we allow for a difference  $\Delta X_0$  in the initial protocol position  $X(t_0)$  and initial true position  $\phi(t_0)$  of the wave,

$$\phi(t_0) = ct_0 \equiv \phi_0, \quad (18)$$

$$X(t_0) = X_0, \quad (19)$$

$$\Delta X_0 \equiv \phi_0 - X_0. \quad (20)$$

Thus at the initial time  $t = t_0$ , the control is applied not at the current position  $\phi_0$  of the wave but rather at a different position  $X_0 = \phi_0 - \Delta X_0$ . We introduce the function  $\Delta X$  as the difference between true and intended position of the traveling wave,

$$\Delta X(ct - X(t)) = \phi(t) - X(t). \quad (21)$$

We consider stability against a perturbed initial condition  $\Delta X_0 \neq 0$  by analyzing the time evolution of  $\Delta X$ . If  $\Delta X$  increases or decreases without bounds in finite or infinite time,

$$\max_{t \in (t_0, \infty)} \Delta X(ct - X(t)) = \pm\infty, \quad (22)$$

the control is considered unstable. If it decreases to zero or increases only up to a finite value

$$\max_{t \in (t_0, \infty)} |\Delta X(ct - X(t))| \leq b, \quad 0 \leq b < \infty, \quad (23)$$

the control is considered stable. Thus we allow the traveling wave to lag behind or move ahead the protocol as long as their displacement  $\Delta X$  remains bounded in time. It is in that sense that we are able to speak about stability of position control on the level of the equation of motion.

Using the difference between the position of the unperturbed traveling wave and protocol  $z(t) = ct - X(t)$

as the new coordinate, an ODE for  $\Delta X$  can be derived which does not depend explicitly on the protocol  $X(t)$ ,

$$\begin{aligned} \Delta X'(z) &= 1 - \frac{1}{K_c} \int_{-\infty}^{\infty} dx \mathbf{W}^{\dagger T}(x) \mathcal{G}(\mathbf{U}_c(x)) \\ &\quad \mathcal{G}^{-1}(\mathbf{U}_c(x + \Delta X(z))) \mathbf{U}'_c(x + \Delta X(z)). \end{aligned} \quad (24)$$

Here, the prime denotes the derivative with respect to  $z$ . According to (20),  $z(t_0) = \Delta X_0$  and hence the initial condition for  $\Delta X$  reads

$$\Delta X(\Delta X_0) = \Delta X_0. \quad (25)$$

It turns out that the argument of the initial condition determines the value of the latter itself. The stability of position control is entirely determined by the ODE for  $\Delta X$ , Eq. (24), together with the initial condition Eq. (25).

An obvious stationary point  $\Delta X_1$  of Eq. (24) is  $\Delta X = \Delta X_1 \equiv 0$

$$\Delta X'(z) = 1 - \underbrace{\frac{1}{K_c} \int_{-\infty}^{\infty} dx \mathbf{W}^{\dagger T}(x) \mathbf{U}'_c(x)}_{=K_c} = 0. \quad (26)$$

This stationary point corresponds to the control function Eq. (13) found as a solution to the integral equation Eq. (5). The behavior of  $\Delta X$  near to the  $\Delta X = 0$  is determined by the linear growth rate  $\lambda_1$ ,

$$\begin{aligned} \lambda_1 &= -\frac{1}{G_c} \int_{-\infty}^{\infty} dx \mathbf{W}^{\dagger T}(x) [\mathbf{U}''_c(x) + \\ &\quad \mathcal{G}(\mathbf{U}_c(x)) \mathcal{G}^{-1}(\mathbf{U}_c(x)) \mathbf{U}'_c(x)^2], \end{aligned} \quad (27)$$

which arises upon a linearization of Eq. (24) around  $\Delta X = 0$ ,

$$\Delta X'(z) = \lambda_1 \Delta X(z) + \mathcal{O}(\Delta X(z)^2). \quad (28)$$

The solution of the linearized equation Eq. (28) is

$$\Delta X(z) = \Delta X_0 e^{\lambda_1(z - \Delta X_0)}. \quad (29)$$

If Eq. (24) would be a dynamical system, we could prove the stability or instability of the trivial stationary point  $\Delta X = 0$  by determining the properties of the linear growth rate  $\lambda_1$ . The problem is that the coordinate  $z(t) = ct - X(t)$  is not a time-like coordinate: contrary to time  $t$ , which always increases from an initial value  $t = t_0$  to  $t \rightarrow \infty$ ,  $z$  can also decrease. Thus the ODE which determines stability, Eq. (24), cannot be seen as a dynamical system, and a positive linear growth rate,  $\lambda_1 > 0$ , of a stationary point does not necessarily imply its instability. To address this problem, we distinguish three different types of protocols.



1. Decelerating protocols. These protocols are slower than the velocity  $c$  of the uncontrolled wave for all times  $t > t_0$  such that  $\dot{z}(t) = c - \dot{X}(t) > 0$  and so

$$\begin{aligned} \lim_{t \rightarrow \infty} z(t) &= \int_{t_0}^{\infty} dt \dot{z}(t) + \Delta X_0 \\ &= \int_{t_0}^{\infty} dt (c - \dot{X}(t)) + \Delta X_0 = \infty. \end{aligned} \quad (30)$$

$z$  is increasing indefinitely with time and it is thus a time-like coordinate, and the first order ODE Eq. (24) can be seen as a usual dynamical system evolving forward in time.

2. Accelerating protocols. Such protocols are faster than the velocity  $c$  of the uncontrolled wave for all times such that  $\dot{z}(t) = c - \dot{X}(t) < 0$  and so

$$\lim_{t \rightarrow \infty} z(t) = \lim_{t \rightarrow \infty} ct - X(t) = -\infty. \quad (31)$$

$z$  is decreasing indefinitely with time and it is thus behaving opposite to a time-like coordinate. The first order ODE Eq. (24) must be seen as a dynamical system evolving backward in time.

3. Protocols which are neither accelerating nor decelerating. Examples are protocols which are alternatingly faster and slower than the velocity  $c$  of the unperturbed wave.

It is well known, that stationary points of a dynamical system change their stability properties under time reversal: a stable stationary point becomes unstable under time reversal and vice versa for an unstable stationary point, see e.g. [33].

It immediately follows that if the linear growth rate is e.g.  $\lambda_1 > 0$ , the stationary point  $\Delta X = 0$  is unstable for decelerating protocols, while it is stable for accelerating protocols. However, numerical simulations of controlled RDS show that position control works for accelerating as well as decelerating protocols. We will find that apart from the trivial stationary point at  $\Delta X_1 = 0$ , other stationary points can exist which essentially stabilize decelerating protocols.

In the following, we investigate only the simplest case with a coupling matrix equal to the identity,  $\mathcal{G} = \mathbf{1}$ . The equation for  $\Delta X$  is given by the convolution of the Goldstone mode with the adjoint Goldstone mode,

$$\Delta X'(z) = 1 - \frac{\int_{-\infty}^{\infty} dx \mathbf{W}^{\dagger T}(x) \mathbf{U}'_c(x + \Delta X(z))}{\int_{-\infty}^{\infty} dx \mathbf{W}^{\dagger T}(x) \mathbf{U}'_c(x)}. \quad (32)$$

Because traveling wave profiles  $\mathbf{U}_c(x)$  are localized in the sense of Eq. (3), it follows

$$\lim_{\Delta X \rightarrow \pm\infty} \Delta X'(z) = 1. \quad (33)$$

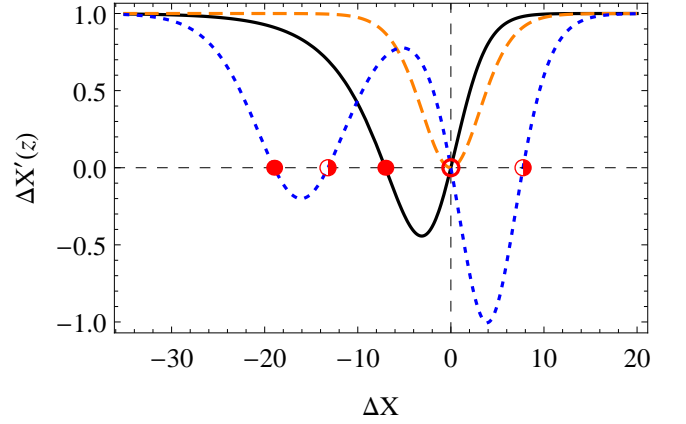


Figure 1. Possible scenarios for stability of position control.  $\Delta X'(z)$  as a function of  $\Delta X$  connects the stationary point  $\Delta X = 0$  (circle) at the origin with 1 as  $\Delta X \rightarrow \pm\infty$  and exhibits one (black line) or several (blue dotted line) minima. Minima with  $\Delta X' < 0$  lie between two stationary points with alternating stability (disks/half-open disks) given by the slope of  $\Delta X'$  at the stationary point. The origin can be degenerate such that two stationary points coalesce in a single minimum (dashed orange line).

Thus the r.h.s of Eq. (32) as a function of  $\Delta X$  connects 1 as  $\Delta X \rightarrow \pm\infty$  with the stationary point  $\Delta X = 0$  at the origin, as it is schematically depicted in Fig. 1. It follows that there must be a minimum of  $\Delta X'(z)$  near to or at the origin. In general, apart from the trivial stationary point at the origin  $\Delta X = 0$ , a second stationary point exists at  $\Delta X = \Delta X_2$  left or right to the origin (black line and blue dotted line in Fig. 1). The origin might be a degenerated stationary point such that two stationary points coalesce at a minimum of  $\Delta X'(z)$  such that  $\Delta X_2 = 0$  (orange dashed line). It is possible that more than two stationary points exist which implies that there is more than one minimum (blue dotted line). In the following we assume the generic case that no more than two stationary points exist. The position of the second stationary point  $\Delta X_2$  can be estimated by expanding the equation for  $\Delta X$ , Eq. (32), up to second order

$$\Delta X'(z) = \lambda_1 \Delta X(z) + \lambda_2 \Delta X(z)^2 + \mathcal{O}(\Delta X(z)^3). \quad (34)$$

The linear and nonlinear growth rate  $\lambda_1$  and  $\lambda_2$  respectively are given as

$$\lambda_1 = -\frac{\int_{-\infty}^{\infty} dx \mathbf{W}^{\dagger T}(x) \mathbf{U}''_c(x)}{\int_{-\infty}^{\infty} dx \mathbf{W}^{\dagger T}(x) \mathbf{U}'_c(x)}, \quad (35)$$

$$\lambda_2 = -\frac{1}{2} \frac{\int_{-\infty}^{\infty} dx \mathbf{W}^{\dagger T}(x) \mathbf{U}'''_c(x)}{\int_{-\infty}^{\infty} dx \mathbf{W}^{\dagger T}(x) \mathbf{U}'_c(x)}. \quad (36)$$

Because the extremum next to the origin is a minimum, the coefficient  $\lambda_2$  must be positive.  $\Delta X_2$  is given by the

quadratic approximation Eq. (34) as

$$\Delta X_2 \approx -\frac{\lambda_1}{\lambda_2} = -2 \frac{\int_{-\infty}^{\infty} dx \mathbf{W}^{\dagger T}(x) \mathbf{U}_c''(x)}{\int_{-\infty}^{\infty} dx \mathbf{W}^{\dagger T}(x) \mathbf{U}_c'''(x)}. \quad (37)$$

Stationary points have alternating stability properties given by the slope of  $\Delta X'(z)$  at the stationary point, which is indicated by full and half-open disks in Fig. 1, respectively. If the linear growth rate of  $\Delta X = 0$  is positive,  $\lambda_1 > 0$ , then the linear growth rate  $\tilde{\lambda}_1$  of  $\Delta X_2$  must be  $\tilde{\lambda}_1 < 0$ . Within the quadratic approximation of Eq. (34), we obtain  $\tilde{\lambda}_1 = -\lambda_1$ .

The crucial point for the stability of position control is now the following observation: if the initial condition  $\Delta X_0$  of  $\Delta X(z)$  lie in a region bounded by two stationary points, this region can never be left. The dynamics of Eq. (32) cannot jump across the stationary points and position control is stable independent of the type of protocol. Outside of that region, the dynamics of Eq. (32) depends on the type of protocol.

In the next sections, we analyze two simple but representative reaction-diffusion models in detail. We will show that the qualitative picture sketched above of the dynamics leading to a successful position control can indeed be found in these models.

## V. SINGLE COMPONENT MODELS

First we consider single component models. The adjoint Goldstone mode  $W^\dagger(\xi)$  can be expressed in terms of the Goldstone mode as

$$W^\dagger(\xi) = e^{c\xi/D} U_c'(\xi). \quad (38)$$

The growth rate  $\lambda_1$  Eq. (35) of the trivial stationary point at  $\Delta X = 0$  follows by partial integration as

$$\lambda_1 = \frac{c}{2D}. \quad (39)$$

This result is universal for any single component model and depends on the reaction kinetics solely through the velocity  $c$ . In the remainder of this subsection, we assume that  $c > 0$ , which implies  $\lambda_1 > 0$ .

Below, we analyze the ODE for the stability Eq. (32), for the case of the Schlögl model, where a traveling front solution is known analytically. The Schlögl model [34], also known as bistable model or Zeldovich-Frank-Kamenetskii equation [35], is a single-component RDS with a cubic reaction function. In rescaled form, the reaction term reads

$$R(u) = -u(u-a)(u-1). \quad (40)$$

The traveling wave profile  $U_c(\xi)$  is a heteroclinic connection between the larger homogeneous steady state  $u = 1$  for  $\xi \rightarrow -\infty$  and the lower one at  $u = 0$  for  $\xi \rightarrow \infty$  [36]

$$U_c(\xi) = \frac{1}{1 + \exp\left(\frac{\xi}{\sqrt{2}}\right)}. \quad (41)$$

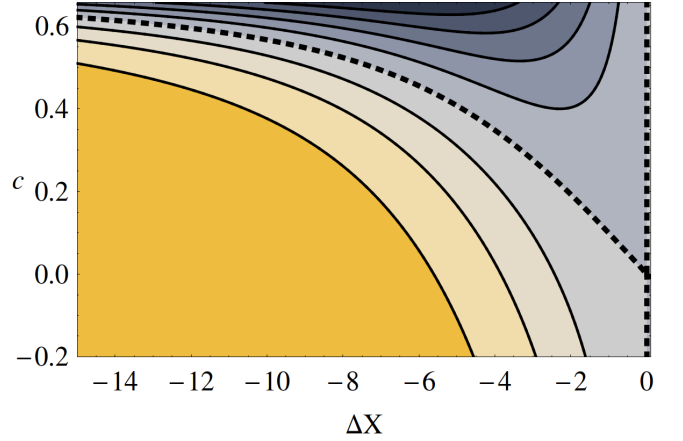


Figure 2.  $\Delta X'(z)$  as a function of velocity  $c$  and  $\Delta X$  for the Schlögl model, see the r.h.s of Eq. (43). Stationary points,  $\Delta X'(z) = 0$ , are indicated by black dotted lines. These lines separate the regions where  $\Delta X'(z) > 0$  (bright) and  $\Delta X'(z) < 0$  (dark). Eq. (43) is invariant under the combined transform of  $\Delta X \rightarrow -\Delta X$  and  $c \rightarrow -c$  and therefore the figure is invariant under inversion with respect to the origin.

This front solution travels with a velocity

$$c = \frac{1}{\sqrt{2}} (1 - 2a). \quad (42)$$

In contrast to the front velocity, the front profile  $U_c(\xi)$  does not depend on the system parameter  $a$ . This is a peculiarity of the Schlögl model.

By means of Eq. (41), the integrals arising in the ODE for  $\Delta X(z)$ , Eq. (32), can be computed exactly,

$$\begin{aligned} \Delta X'(z) = 1 + & \frac{6e^{\frac{(a+1)\Delta X}{\sqrt{2}}}}{a(a-1)(2a-1) \left(e^{\frac{\Delta X}{\sqrt{2}}} - 1\right)^3} \\ & \times \left( a \sinh\left(\frac{(a-1)\Delta X}{\sqrt{2}}\right) - (a-1) \sinh\left(\frac{a\Delta X}{\sqrt{2}}\right) \right). \end{aligned} \quad (43)$$

The result is given in terms of the single system parameter  $a$  of the Schlögl model. But since there is one-to-one mapping between  $a$  and the velocity  $c$ , see Eq. (42), it can easily be expressed in terms of the velocity.

Fig. 2 shows the r.h.s of Eq. (43) as a function of  $\Delta X$  and velocity  $c$ . It demonstrates that apart from the stationary point at  $\Delta X = \Delta X_1 = 0$  (marked by the black dashed line), a second stationary point at  $\Delta X = \Delta X_2$  exists.  $\Delta X_2$  being the solution to a transcendental equation, cannot be determined analytically. The position of the second stationary point  $\Delta X_2$  depends on the system parameter  $a$ . For  $0 < a < 1/2$  and so  $c > 0$ , this point is found at  $\Delta X_2 < 0$ , while for  $1/2 < a < 1$  and so  $c < 0$ , it is found at  $\Delta X_2 > 0$ . For  $a = 1/2$  and so  $c = 0$ , both stationary points coalesce in a minimum of  $\Delta X'(z)$  at  $\Delta X_2 = \Delta X_1 = 0$ . In the limit of  $a \rightarrow 0$ , the velocity  $c$  approaches its largest possible value  $c \rightarrow 1/\sqrt{2}$  and

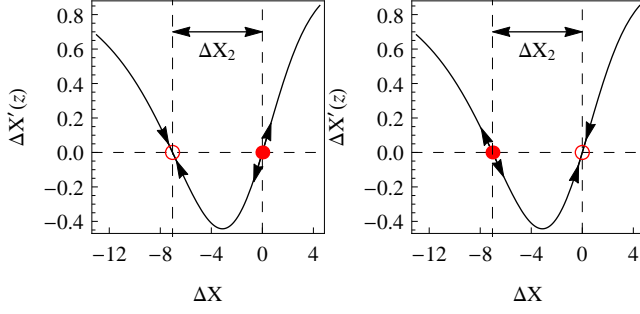


Figure 3. Possible scenarios for stability of position control in the Schlögl model.  $\Delta X'(z)$  as a function of  $\Delta X$  for parameter  $a = 0.15$ , which corresponds to a velocity  $c = (1 - 2a)/\sqrt{2} = 0.495$ . Left: For decelerating protocols, the unstable stationary point (red dot) is  $\Delta X = 0$  while the stable one (red circle) is at  $\Delta X = \Delta X_2 \approx -7.04$ . An initial condition  $\Delta X (\Delta X_0) = \Delta X_0 > 0$  will lead to  $\Delta X$  increasing to infinity. For  $\Delta X_0 < 0$ ,  $\Delta X$  will decrease until it reaches the second stable stationary point. Right: For accelerating protocols, the stationary point at  $\Delta X = 0$  is stable, the other one is unstable.

the position of the second stationary point approaches  $\Delta X_2 \rightarrow -\infty$ . Eq. (43) is invariant under the combined transform of  $\Delta X \rightarrow -\Delta X$  and  $c \rightarrow -c$ .

Fig. 3 shows a cross section of Fig. 2 for a fixed value of the velocity  $c$ . The stable (red dot) and unstable (red circle) stationary points are shown. The stability of  $\Delta X_2$  is contrary to that at  $\Delta X_1 = 0$ : if  $\Delta X_1$  is stable,  $\Delta X_2$  is unstable, and vice versa.

Knowing the position and stability properties of the stationary points of Eq. (43), we can state the following. Consider a wave traveling to the right, i.e.  $c > 0$  and an accelerating protocol such that  $\Delta X_1 = 0$  is stable. While a perturbation of the initial condition with  $\Delta X_0 > 0$  is unconditionally stable, a perturbation of the initial condition with  $\Delta X_0 < 0$  is stable only as long as  $|\Delta X_0|$  does not exceed the distance  $|\Delta X_2|$  between the stationary point,  $|\Delta X_0| < |\Delta X_2|$ . On the other hand, if the initial perturbation is larger, i.e.  $|\Delta X_0| > |\Delta X_2|$ , then the difference  $\Delta X(t)$  between protocol  $X(t)$  and true wave position  $\phi(t)$  will grow unboundedly.

Physically, this dependence on the initial conditions can be understood as follows. If the initial perturbation is  $\Delta X_0 = \phi_0 - X_0 > 0$ , the control is initially applied to the left of the wave's position. Because the protocol is accelerating and thus moving faster than the wave, the control will eventually catch up with the wave and be able to hold it, see Fig. 4 for a sketch of this scenario. Conversely, if  $\Delta X_0 = \phi_0 - X_0 < 0$ , the control is initially applied in front of the wave and moving away from it. As long as  $\Delta X_0$  is small enough, such a perturbation will not lead to the loss of control of the wave's position. But if the control is initially applied outside the region of stability of the wave such that  $|\Delta X_0| > |\Delta X_2|$  and additionally moving away from the wave, the control is not able to catch up with the traveling wave and position

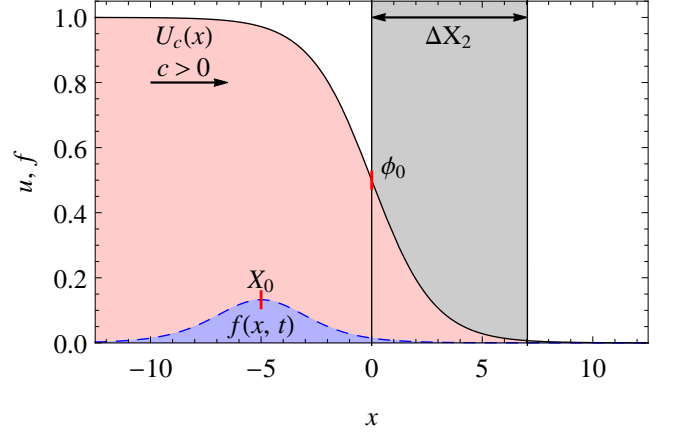


Figure 4. The stability analysis identifies a region of stability (shaded region) of a traveling wave (black solid line). Control (blue dashed) is initially applied to the left of this region, thus  $\Delta X_0 = \phi_0 - X_0 > 0$  and position control can be unstable. If the protocol is decelerating, the control is moving slower than velocity  $c$  of the wave and position control is unstable. If the protocol is accelerating and control is moving faster than the wave, it will eventually catch up with the wave and position control is stable.

control will eventually fail.

A slightly different scenario occurs for decelerating protocols since the stationary point  $\Delta X_1 = 0$  is unstable. For positive initial perturbations,  $\Delta X_0 > 0$ ,  $\Delta X(t)$  will increase without bounds and we have an unstable situation. If the initial condition  $\Delta X_0 < 0$ ,  $\Delta X(t)$  will decrease until it reaches the stationary point  $\Delta X = \Delta X_2$  which is stable.

We conclude that our proposed position control is stable against initial perturbations  $\Delta X_0$  simultaneously for accelerating as well as decelerating protocols if  $\Delta X_0$  lies between the two stationary points. For positive as well as negative values of  $\Delta X_2$ , this can be expressed as

$$|\Delta X_2| > |\Delta X_0| > \Delta X_1 = 0, \quad (44)$$

$$\text{sign}(\Delta X_0) = \text{sign}(\Delta X_2), \quad (45)$$

where  $\text{sign}(x)$  denotes the sign of  $x$ . The same is true for protocols which are neither accelerating nor decelerating.  $\Delta X(t)$  will just move back and forth along the line connecting the two stationary points and will never cross them. As long as the linear growth rate near to the stationary points is nonzero, stationary points cannot be reached in finite time because the dynamics near to the stationary points becomes exponentially slow. Therefore, initial perturbations  $\Delta X_0$  lying inside the region of stability will never leave this region.

Simultaneously, the region of stability Eq. (44) identifies an upper limit of accuracy for position control. For a general protocol, we can only guarantee that the intended wave position as given by the protocol  $X$  lies within the stability region, but the wave's true position  $\phi$  might differ by the value  $|\Delta X| < |\Delta X_2|$  from  $X$ .

It is imaginable that numerical simulations or experi-

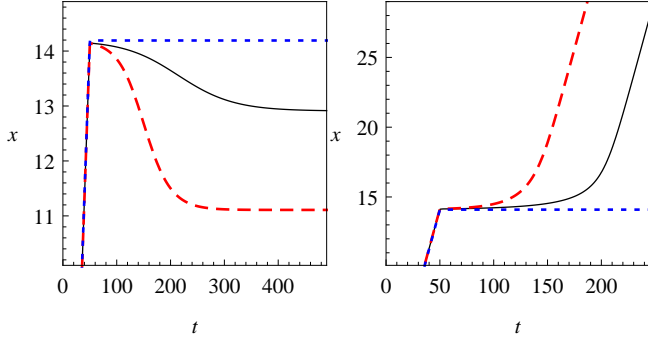


Figure 5. Space-time plot of the front evolution under position control demonstrating the instability of the stationary point  $\Delta X = 0$  for decelerating protocols. Blue dotted line: protocol  $X(t)$  which drives the propagation velocity smoothly to zero. Black line: trajectory of controlled Schlögl model for  $u(x, t) = 1/2$ . Red dashed line: solution  $\phi(t)$  of the equation of motion. Left shows a stable situation arising for an initial perturbation  $\Delta X_0 = -0.05$ . Right demonstrates the unstable case for an initial perturbation of  $\Delta X_0 = 0.05$ . See supplemental material [37] for movies.

ments with controlled RDS, even when starting with an initial perturbation  $\Delta X_0 = 0$ , lead to spontaneous differences  $\delta X$  between protocol and wave's position in the course of time evolution due to noise or deterministic effects which are neglected by the equations of motion. By using the latter, we are unable to predict the sign and value of such a spontaneous difference. Therefore, to compare the result from above with numerical simulations, we will implement the perturbations manually and start with an artificial initial difference  $\Delta X_0$  between protocol and wave position.

In the following, we demonstrate the behavior found in numerical simulations of the controlled Schlögl model, Eq. (1) with cubic reaction function Eq. (40) and Neumann boundary conditions. The unperturbed traveling wave profile Eq. (41) is used as the initial condition. The position over time of a controlled front solution is defined as the point  $x$  such that the numerical solution  $u(x, t)$  to the controlled Schlögl model equals  $u(x, t) = 1/2$ . We suppose a protocol which drives the velocity smoothly from  $\dot{X}(t_0) = c$  at initial time  $t = t_0$  to a velocity  $c_2$  at a later time,

$$\dot{X}(t) = c_2 + \frac{1}{2}(c - c_2)(\tanh(k(\Delta t - t)) + 1). \quad (46)$$

The corresponding position protocol is obtained by integration and setting  $X(t_0) = X_0$  as

$$X(t) = X_0 + \frac{1}{2}(c + c_2)(t - t_0) - \frac{1}{2k}(c - c_2) \log \left( \frac{\cosh(k(t - \Delta t))}{\cosh(k(t_0 - \Delta t))} \right). \quad (47)$$

The parameter  $k$  controls the slope of the transition occurring at  $t = \Delta t$ . In all numerical simulations, we

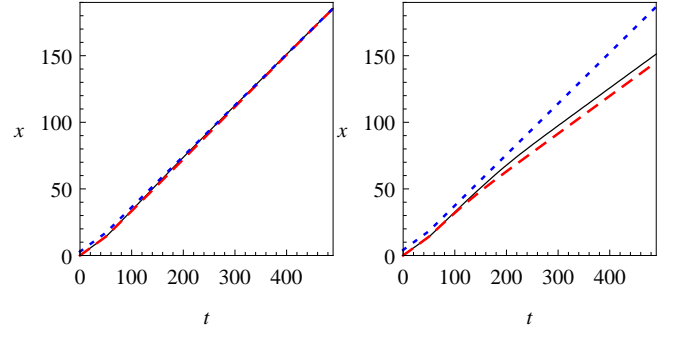


Figure 6. Space-time plot of the front evolution under position control demonstrating the instability of the stationary point  $\Delta X = \Delta X_2$  for accelerating protocols upon an overcritical initial perturbation. Blue dotted line: protocol  $X(t)$  which drives the propagation velocity smoothly to  $c_2 = c + 0.1$ . Black line shows the trajectory traced out by the numerical solution of the controlled RDS for  $u(x, t) = 1/2$ . Red dashed line: solution  $\phi(t)$  of the equation of motion. Left shows an undercritical initial perturbation  $\Delta X_0 = 0.95\Delta X_2$ . Right demonstrates the unstable case for an overcritical initial perturbation of  $\Delta X_0 = 1.35\Delta X_2$ . See supplemental material [37] for movies.

use  $k = 2$  and  $\Delta t = 50$ . The single parameter  $a$  of the Schlögl model is chosen as  $a = 0.3$  such that  $c = (1 - 2a)/\sqrt{2} = 0.282 > 0$ .

Fig. 5 compares the time evolution of the controlled Schlögl model with that predicted by the equation of motion Eq. (17) with  $\mathcal{G} = 1$ . We use a decelerating protocol, Eq. (47), with  $c_2 = 0$  such that the front is stopped. In agreement with the equation of motion (red dashed line), the difference between protocol  $X(t)$  (blue dotted line) and actual wave position  $\phi(t)$  (black line) grows unboundedly if  $\Delta X_0$  lies outside the region of stability (see Fig. 5 right). On the other hand, if  $\Delta X_0$  lies inside the region of stability (see Fig. 5 left), the front is stopped. However, it is not stopped at the position predicted by the protocol  $X(t)$ , but at a slightly different position, thus confirming the existence of a second stationary point at  $\Delta X = \Delta X_2$ . So we conclude that the stationary point  $\Delta X_1 = 0$  is unstable for a decelerating protocol, while the stationary point  $\Delta X_2$  is stable.

Fig. 6 shows the results for an accelerating protocol, Eq. (47), which increases the velocity from  $c$  to  $c_2 = c + 0.1$ . In Fig. 6 left, the initial perturbation  $\Delta X_0 = 0.95\Delta X_2$  is undercritical and the wave will ultimately follow the protocol. As demonstrated in Fig. 6 right, an overcritical perturbation  $\Delta X_0 = 1.35\Delta X_2$  will lead to a difference  $\Delta X$  between protocol and true wave position growing indefinitely in time. For late times, the wave will travel with the velocity  $c$  of the unperturbed case. Thus we demonstrated the instability of the stationary point  $\Delta X_2$  and the possibility of overcritical perturbations for an accelerating protocol.

The position of the second stationary point  $\Delta X_2$  predicted by the equation of motion,  $\Delta X_2 \approx -3.1$  differs from the stationary point  $\Delta X_2^{\text{num}}$  found by numerical



simulations of the controlled Schlögl model. Furthermore, contrary to the prediction by the equation of motion, the position of  $\Delta X_2$  depends on the type of protocol. For the decelerating case it appears at a smaller distance  $\Delta X_2^{\text{num}} \approx \frac{1}{3}\Delta X_2$ , as can be estimated from Fig. 5 left. For the accelerating protocol, it is found roughly at  $\Delta X_2^{\text{num}} \approx 1.25\Delta X_2$ . Nevertheless, qualitatively, the dynamics on the level of the reaction-diffusion system agrees with that found on the level of the equation of motion.

## VI. MULTICOMPONENT MODELS

According to Kuramoto [38, 39], the following identity is valid for all reaction-diffusion systems:

$$\frac{\int_{-\infty}^{\infty} dx \mathbf{W}^{\dagger T}(x) D \mathbf{U}_c''(x)}{\int_{-\infty}^{\infty} dx \mathbf{W}^{\dagger T}(x) \mathbf{U}_c'(x)} = -\frac{c}{2}. \quad (48)$$

If  $D$  is equal for all components, then

$$D = \hat{D} \mathbf{1} \quad (49)$$

and

$$\frac{\int_{-\infty}^{\infty} dx \mathbf{W}^{\dagger T}(x) D \mathbf{U}_c''(x)}{\int_{-\infty}^{\infty} dx \mathbf{W}^{\dagger T}(x) \mathbf{U}_c'(x)} = -\hat{D} \lambda_1 = -\frac{c}{2}. \quad (50)$$

Thus, for the case of equal diffusion coefficients, we obtain a universal result for the linear growth rate of the trivial stationary point  $\Delta X = 0$

$$\lambda_1 = \frac{c}{2\hat{D}} > 0, \quad (51)$$

independent of the details of the reaction kinetics. Thus, we expect that only if the diffusion coefficients are very different from each other,  $\lambda_1$  can be zero or change sign. As a representative example, we consider the FitzHugh-Nagumo model [40, 41]

$$\partial_t u = D_u \partial_x^2 u + f_1(u) - v + \epsilon f_u, \quad (52)$$

$$\partial_t v = D_v \partial_x^2 v + \tilde{\epsilon}(u - \delta) - \tilde{\epsilon}\gamma v + \epsilon f_v, \quad (53)$$

with

$$f_1(u) = 3u - u^3. \quad (54)$$

This model has a stable traveling pulse solution whose shape and velocity is nevertheless not analytically known. Hence, we resort to the numerical computation of the traveling wave solution  $\mathbf{U}_c(x)$  as well as the Goldstone mode  $\mathbf{U}_c'(x)$  and the response function  $\mathbf{W}^\dagger(x)$ .

Fig. 7 shows the the r.h.s. of Eq. (32) as a function of  $\Delta X$ . On a large scale, this function looks very different from the case of the Schlögl model: there are two local minima and a maximum. However, the closeup of

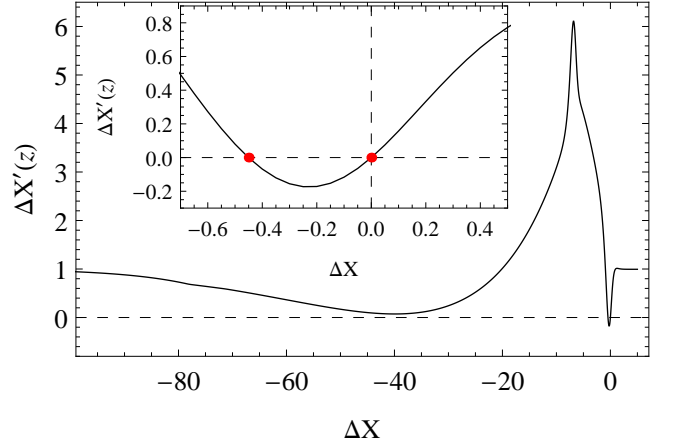


Figure 7.  $\Delta X'(z)$  as a function of  $\Delta X$  for a traveling pulse in the FitzHugh-Nagumo model. System parameters are  $D_u = D_v = 0.2$ ,  $\epsilon = 0.1$ ,  $\delta = -1.3$ . Inset shows closeup of the region near to the origin which is crucial for position control. Although on large scales  $\Delta X'(z)$  looks very different when compared to the Schlögl model, the closeup reveals the characteristic features necessary for stable position control, i.e. two stationary points with an intermediate minimum.

the region near to the origin depicted in the inset of Fig. 7 reveals a situation very similar to the Schlögl model. Again, we find two stationary points; one of which is stable and one of which is unstable. Because the fate of position control is decided in this region near to the origin, we conclude that the qualitative properties of position control in the Schlögl model also apply in this case. Note that in general there could be additional stationary points further away from the origin. This is indicated by the second local minimum in Fig. 7 which could cross the axis  $\Delta X'(z) = 0$  upon a change of parameters. Additional stationary points necessarily have alternating slopes such that they are stable or unstable depending on the type of protocol. Therefore, in principle, there could be more than one region of stability for initial perturbations.

## VII. STABILITY OF POSITION CONTROL OF STATIONARY SOLUTIONS

The stability properties of position control of stationary solutions  $U_0(x)$  to single component reaction-diffusion systems are different. Since the velocity  $c$  equals zero, the universal linear growth rate  $\lambda_1$  as given by Eq. (39) for single component models vanishes,  $\lambda_1 = 0$ . For general multicomponent models, there is no simple expression for the linear growth rate  $\lambda_1$ , and we must analyze the general expression

$$\lambda_1 = -\frac{\int_{-\infty}^{\infty} dx \mathbf{W}^{\dagger T}(x) \mathbf{U}_0''(x)}{\int_{-\infty}^{\infty} dx \mathbf{W}^{\dagger T}(x) \mathbf{U}_0'(x)} \quad (55)$$

with  $\mathbf{W}^\dagger$  given as the solution of Eq. (8) with adjoint operator  $\mathcal{L}^\dagger$ , Eq. (9), for  $c = 0$ . In appendix B, we prove that the linear growth rate  $\lambda_1$  vanishes identically for stationary solutions  $\mathbf{U}_0(x)$  exhibiting a reflection symmetry

$$\mathbf{U}_0(x) = \mathbf{U}_0(-x). \quad (56)$$

For all solutions with  $\lambda_1 = 0$  we have the case of a degenerate stationary point at the origin, depicted by the orange dashed line in Fig. 1: both stationary points  $\Delta X = 0$  and  $\Delta X = \Delta X_2$  coalesce in a single stationary point at the origin. Moreover,  $\Delta X = 0$  is also a minimum of  $\Delta X'(z)$ . To determine the stability of the stationary point  $\Delta X = 0$ , the expansion of Eq. (24) for small  $\Delta X$  needs to be carried further

$$\Delta X'(z) = \lambda_2 \Delta X(z)^2 + \mathcal{O}(\Delta X(z)^3). \quad (57)$$

For single component models, the nonlinear growth rate  $\lambda_2$  is a positive quantity,

$$\begin{aligned} \lambda_2 &= -\frac{1}{2K_c} \int_{-\infty}^{\infty} dx U_0'(x) U_0'''(x) \\ &= \frac{1}{2} \frac{\int_{-\infty}^{\infty} dx (U_0''(x))^2}{\int_{-\infty}^{\infty} dx (U_0'(x))^2} > 0. \end{aligned} \quad (58)$$

For all multicomponent models,  $\lambda_2$  is determined as

$$\begin{aligned} \lambda_2 &= -\frac{1}{2K_c} \int_{-\infty}^{\infty} dx \mathbf{W}^{\dagger T}(x) \mathbf{W}''(x) \\ &= \frac{1}{2} \frac{\int_{-\infty}^{\infty} dx \mathbf{W}^{\dagger T'}(x) \mathbf{U}_0''(x)}{\int_{-\infty}^{\infty} dx \mathbf{W}^{\dagger T}(x) \mathbf{U}_0'(x)}. \end{aligned} \quad (59)$$

Positivity of  $\lambda_2$  follows because the stationary point  $\Delta X = 0$  is a minimum.

The solution of Eq. (57) with initial condition Eq. (25) is

$$\Delta X(z) = \frac{\Delta X_0}{1 + \Delta X_0 (\Delta X_0 - z) \lambda_2}. \quad (60)$$

It diverges at a finite value  $z = z_\infty$  where

$$z_\infty = \Delta X_0 + \frac{1}{\lambda_2 \Delta X_0}. \quad (61)$$

If the value of  $z = z_\infty$  is actually reached during time evolution depends on the type of protocol and the value of the initial perturbation. Remember that for a decelerating protocol,  $z$  is growing with time from  $z = \Delta X_0$  to  $z = \infty$ , while for an accelerating protocol,  $z$  is decreasing from  $z = \Delta X_0$  to  $z = -\infty$ . If  $\Delta X_0 < 0$  then  $z_\infty < \Delta X_0$  and so  $z$  does not assume the value  $z = z_\infty$  for the case of a decelerating protocol. This corresponds to stable position control because the difference between protocol  $X(t)$  and actual position of the wave  $\phi(t)$  decays to 0 as  $z \rightarrow \infty$  and does not diverge for a finite

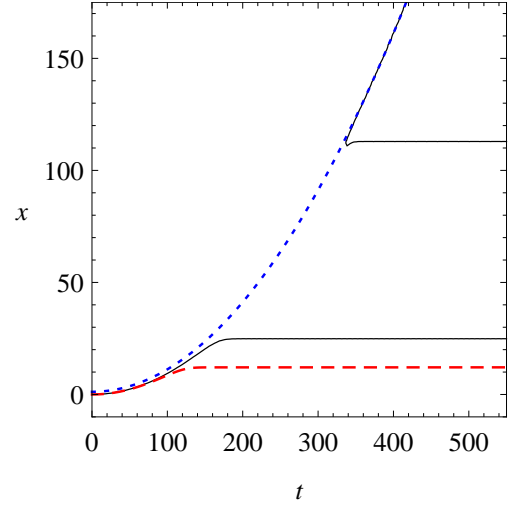


Figure 8. Position control of stationary front solution to the Schlögl model. Blue dotted line: protocol  $X(t)$  accelerating the wave. Black line shows the trajectory traced out by the numerical solution of the controlled RDS for  $u(x, t) = 1/2$ . Red dashed line: solution  $\phi(t)$  of the equation of motion. For the initial condition  $\Delta X_0 = -1.2$ , position control is unstable. After some time the control is large enough such that a new front is excited, see black triangular line in the upper right corner and movie [37].

value of  $z$ . However,  $\Delta X(z)$  diverges for a finite value of  $z$  in the case of an accelerating protocol and  $\Delta X_0 < 0$ . We conclude that position control is stable for negative initial perturbations  $\Delta X_0 < 0$  and decelerating protocols and positive initial perturbations  $\Delta X_0 > 0$  and accelerating protocols. However, there is no region of stability where accelerating and decelerating protocols are simultaneously stable. Therefore a region of stability does not exist. If position control of stationary solutions is stable, decay of an initial perturbation  $\Delta X_0$  is only algebraic in contrast to exponential decay in the case of traveling waves with  $c \neq 0$ .

In Fig. 8, we show the position over time plot obtained by numerical simulations of the controlled stationary Schlögl front solution. The system parameter  $a$  must be  $a = 1/2$  such that the velocity  $c = 0$ . An accelerating protocol with  $X(t) = t^2/1000$  is applied. Initially, the position of the front (black line) follows the protocol (blue dotted line), but eventually position control fails. The equation of motion (red dashed line) predicts a qualitatively similar behavior. We chose a rather large value for the initial perturbation  $\Delta X_0 = -1.2$  because for smaller values it can last very long until an instability develops such that it is difficult to find in numerical simulations of the controlled front solution.

As we already mentioned, the region of stability predicted by the equation of motion can differ from the region of stability found in numerical simulations of the controlled RDS. In principle, it could be possible to find a stability region in numerical simulations of controlled stationary

solutions. However, even if it exists, we expect this region to be small. By means of a continuity argument, one can state that as the velocity  $c$  of a traveling wave approaches zero, its profile will become less and less asymmetric until it finally assumes a reflection symmetric profile. At least as long as the velocity  $|c|$  is small, we expect that lowering the velocity  $|c|$  even further should decrease the value of  $|\lambda_1|$  and  $|\Delta X_2|$ , and therefore shrink the size of the region of stability.

Fig. 8 demonstrates another effect of position control which is not predicted by the equation of motion Eq. (5). The amplitude of the control function increases without bounds in time because the protocol velocity grows linearly,  $\dot{X}(t) \sim t$ . At a certain moment  $t_1$ , the amplitude of the control function becomes too large and triggers a new front. This new wave follows the protocol for all times  $t > t_1$ . The movie provided in the supplementary material [37] shows this effect in detail. Effects like the nucleation or triggering of new waves always interfere with position control and can have a stabilizing or destabilizing effect.

## VIII. CONCLUSIONS

We study the stability of the position control for traveling waves in reaction-diffusion systems. A general stability analysis valid for arbitrary RDS on the level of the full RDS is futile. Thus we investigate stability on the level of the equations of motion for traveling waves Eq. (5). In particular, we analyze the evolution of the difference  $\Delta X = \phi - X$  between the true wave position  $\phi$  and protocol position  $X$  upon a perturbation of the initial conditions  $\Delta X_0 = \phi_0 - X_0 \neq 0$ .

For initial perturbations  $\Delta X_0$  lying in an interval

$$|\Delta X_2| > |\Delta X_0| > \Delta X_1 = 0, \quad (62)$$

$$\text{sign}(\Delta X_0) = \text{sign}(\Delta X_2), \quad (63)$$

position control is unconditionally stable for all types of protocols of movement.  $\Delta X_2$  is a root of the r.h.s of Eq. (32) and can be approximated as

$$\Delta X_2 \approx -2 \frac{\int_{-\infty}^{\infty} dx \mathbf{W}^{\dagger T}(x) \mathbf{U}_c''(x)}{\int_{-\infty}^{\infty} dx \mathbf{W}^{\dagger T}(x) \mathbf{U}_c'''(x)}. \quad (64)$$

Depending on the type of protocol, initial differences  $\Delta X_0$  outside this region of stability can be unstable. The value of  $\Delta X_2$  and thus the size of the stability region depends on the system parameters. There is a tradeoff between stability and accuracy: the larger is the stability region, the more inaccurate is the position control. In general, there can be more than one stability region.

For stationary multicomponent solutions  $\mathbf{U}_0(x)$  with reflection symmetry and all stationary single component solutions follows  $\Delta X_2 = 0$  and both stationary points coalesce in a local minimum at  $\Delta X = 0$ . Depending on the protocol, position control of such stationary solutions

can always be unstable. Contrary to the generic case of traveling waves with nonzero velocity  $c$ , there is no stability region.

Intuitively, it is clear that traveling waves are most susceptible to perturbations in a “region of sensitivity” close to its position. Any perturbation far away from a wave’s position might cause the generation of new waves, but has little effect on the original solitary wave. For a general perturbation, the position and size of the sensitivity region can roughly be characterized as being the set of points  $x$  where the response function  $\mathbf{W}^{\dagger}(x)$  is significantly different from zero. The region of stability found for position control can be interpreted as a precise quantitative estimate for the position and size of this “region of sensitivity”, see Fig. 4. However, for perturbations  $\mathbf{f}$  which do not intend to control the position, the “region of sensitivity” might look different.

Spontaneous perturbations  $\delta X$  of the difference between wave and protocol position  $\Delta X(z)$  can occur due to noise in experiments and numerical simulations or due to deterministic effects neglected by the equations of motion. Spontaneous perturbations  $\delta X$  are undercritical if they are too small for  $\Delta X + \delta X$  to leave the region of stability,

$$0 < |\Delta X(z) + \delta X| < |\Delta X_2|. \quad (65)$$

Of course, the actual value of  $\delta X$  necessary to induce an instability depends on the actual time-dependent value of  $\Delta X(z(t))$ . The susceptibility to perturbations is smaller near to a stationary point if the type of protocol is kept constant because the perturbation  $\delta X$  must be quite large to be overcritical. However, the susceptibility to perturbations  $\delta X$  is larger near to a stationary point if the type of protocol is exchanged and a small perturbation can already be overcritical and destabilize position control.

Numerical simulations of controlled RDS generally confirm our analysis of stability of position control. However, the stability region found in numerical simulations is of different size and depends on the protocol in contrast to that predicted by the equation of motion.

Note that the position of traveling waves is not given a priori but is defined in a rather arbitrary way as e.g. the position of the maximum amplitude of the activator component. If the position of the stationary point  $\Delta X = 0$  can be determined with sufficient accuracy from numerical simulations (i.e. sufficiently independent of the protocol), it could be used as the definition of the position of a traveling wave

Because of many other potentially destabilizing effects not captured by the equation of motion, our stability result must be interpreted as follows. If we find that position control is unstable on the level of the equation of motion, there is a high probability for position control to be unstable on the level of the controlled RDS. Reversing this conclusion is not possible: if position control is stable on the level of the equation of motion, it is not necessarily stable on the level of the controlled RDS.

## ACKNOWLEDGMENTS

J.L. acknowledges financial support through the GRK 1558.

## Appendix A: Nonlinear stability analysis

Consider a dynamical system evolving in time  $t$

$$\dot{x}(t) = F(x(t)) \quad (\text{A1})$$

with initial condition

$$x(t_0) = \tilde{x}. \quad (\text{A2})$$

Suppose we want to study the stability of a stationary solution  $x(t) = x_0$  of the dynamical system Eqs. (A1), (A2) against perturbations. Naturally,  $x_0$  can only be a stationary solution of the time dependent system if  $\tilde{x} = x_0$ .

There can be at least two types of perturbations: a structural perturbation  $F_1$  of the system itself,

$$\dot{x}(t) = F(x(t)) + F_1(x(t)) \quad (\text{A3})$$

and a perturbation  $x_1$  of the initial condition,

$$x(t_0) = x_0 + x_1. \quad (\text{A4})$$

In the following we consider only stability against perturbations of initial conditions such that  $F_1 \equiv 0$ . We introduce a new function

$$\Delta x(t) = x(t) - x_0 \quad (\text{A5})$$

which is the difference between the solution of the unperturbed and the perturbed system.  $\Delta x(t)$  is governed by the equation

$$\frac{d}{dt}\Delta x(t) = F(x_0 + \Delta x(t)), \quad (\text{A6})$$

with initial condition

$$\Delta x(t_0) = x_1. \quad (\text{A7})$$

If the difference  $\Delta x(t)$  increases or decreases without bounds, the stationary solution  $x_0$  is unstable. If  $\Delta x(t)$  approaches zero for  $t \rightarrow \infty$ , the solution is stable. A linear stability analysis essentially assumes that  $\Delta x(t)$  as well as  $x_1$  are of order  $\epsilon$ , with  $0 < \epsilon \ll 1$ ,  $\Delta x(t) = \epsilon \Delta X(t)$ ,  $x_1 = \epsilon X_1$  with  $\Delta X(t) = \mathcal{O}(1)$ ,  $X_1 = \mathcal{O}(1)$ . Expanding in  $\epsilon$  up to  $\mathcal{O}(\epsilon)$  yields

$$\frac{d}{dt}\Delta X(t) = F'(x_0) \Delta X(t) + \mathcal{O}(\epsilon), \quad (\text{A8})$$

$$\Delta X(t_0) = X_1. \quad (\text{A9})$$

The solution is of the linearized equation is

$$\Delta X(t) = X_1 \exp(F'(x_0)(t - t_0)).$$

Therefore, if  $F'(x_0) > 0$ , the solution  $\Delta X(t)$  will increase or decrease in time without bounds and  $x_0$  is an unstable stationary solution of the dynamical system Eq. (A1). One can say that  $x_0$  is unstable against all possible perturbations  $x_1$  of the initial condition. If  $F'(x_0) < 0$ , the solution  $\Delta X(t)$  will approach zero and the system is stable against all possible perturbations  $x_1$  of the initial condition.

A nonlinear stability analysis proceeds differently: it considers the full nonlinear equation Eq. (A6). Also, the assumption of  $\epsilon$ -smallness of  $\Delta x(t)$  and  $x_1$  is dropped. Because of its nonlinearity, there can exist overcritical and undercritical initial perturbations  $x_1$ . Additionally,  $\Delta x(t)$  can diverge in finite time. Furthermore, one can relax the condition of stability:  $x_0$  is considered stable if  $|\Delta x(t)|$  never exceeds a finite value

$$|\Delta x(t)| < b, \quad 0 \leq b < \infty. \quad (\text{A10})$$

The statement of nonlinear stability of the stationary solution  $x_0$  is then:  $x_0$  is stable against the initial perturbation  $x_1$  if  $\max_{t \in (t_0, \infty)} |\Delta x(t)| < b$ . Otherwise, it is unstable. A nonlinear stability analysis is always necessary if  $F'(x_0) = 0$ , but can be simplified by expanding Eq. (A8) up to orders in  $\epsilon$  higher than one.

## Appendix B: Stationary symmetric patterns

We prove that the linear growth rate  $\lambda_1$  of the stationary point  $\Delta X = 0$ ,

$$\lambda_1 = -\frac{\int_{-\infty}^{\infty} dx \mathbf{W}^{\dagger T}(x) \mathbf{U}_0''(x)}{\int_{-\infty}^{\infty} dx \mathbf{W}^{\dagger T}(x) \mathbf{U}_0'(x)}, \quad (\text{B1})$$

is zero for stationary ( $c = 0$ ) solutions  $\mathbf{U}_0(x)$  of arbitrary RDS which exhibit a reflection symmetry,

$$\mathbf{U}_0(x) = \mathbf{U}_0(-x). \quad (\text{B2})$$

Often, but not always, stationary solutions of reaction-diffusion systems exhibit such a symmetry, also called parity symmetry. We assumed that the origin of the coordinate system is chosen to coincide with the point of symmetry of  $\mathbf{U}_0$ . The symmetry can be expressed with the help of the parity operator  $\pi$  defined as [42]

$$\pi f(x) = f(-x), \quad (\text{B3})$$

where  $f$  is an arbitrary function. Reflection symmetry is equivalent to stating that  $\mathbf{U}_0(x)$  is an eigenfunction of the parity operator to eigenvalue 1,

$$\pi \mathbf{U}_0(x) = \mathbf{U}_0(-x) = \mathbf{U}_0(x). \quad (\text{B4})$$

In general, parity eigenfunctions can have eigenvalues  $\pm 1$ . From Eq. (B4) follows, that  $\mathcal{L}$  as well as  $\mathcal{L}^\dagger$  commute with  $\pi$ ,

$$[\mathcal{L}, \pi] = [\mathcal{L}^\dagger, \pi] = 0. \quad (\text{B5})$$



Consider the functions

$$\tilde{\mathbf{W}}(x) = \frac{1}{2}(1 \pm \pi) \mathbf{W}(x) \quad (\text{B6})$$

with  $\mathcal{L}\mathbf{W} = 0$ . Using  $\pi^2 = 1$ , one finds that  $\tilde{\mathbf{W}}$  is a parity eigenfunction to eigenvalue  $\pm 1$ ,

$$\pi \tilde{\mathbf{W}}(x) = \pm \tilde{\mathbf{W}}(x). \quad (\text{B7})$$

But because of Eq. (B5),  $\tilde{\mathbf{W}}$  is also an eigenfunction of  $\mathcal{L}$  to the eigenvalue  $\lambda = 0$ . Furthermore, because this zero eigenvalue is non-degenerate,  $\tilde{\mathbf{W}}$  and  $\mathbf{W}$  are essentially the same function and can only differ by a multiplicative constant.

We conclude that  $\mathbf{W}(x)$  must be a parity eigenstate. Because  $\mathbf{W}(x) = \mathbf{U}'_0(x)$  and  $\mathbf{U}_0(x)$  is a parity eigenstate to eigenvalue  $+1$ , i.e.,  $\mathbf{U}_0$  is an even function,  $\mathbf{W}$  is actually an odd function and thus an eigenstate to the parity operator of eigenvalue  $-1$ .

Similarly, one can prove that the response function  $\mathbf{W}^\dagger$  is an eigenfunction of the parity operator as well,

$$\pi \mathbf{W}^\dagger(x) = \pm \mathbf{W}^\dagger(x). \quad (\text{B8})$$

So far we proved that  $\mathbf{W}(x) = \mathbf{U}'_0(x)$  is an odd function and that  $\mathbf{W}^\dagger(x)$  is an even or an odd function. If  $\mathbf{W}^\dagger(x)$  would be an even function, the constant  $K_c = \int_{-\infty}^{\infty} dx \mathbf{W}^{\dagger T}(x) \mathbf{U}'_0(x)$ , being an infinite integral over an odd function, would be zero. If that would be the case, the equation of motion could not be used, see Eq. (5). Furthermore, the linear growth rate  $\lambda_1$  itself would be infinite because  $K_c$  appears in the denominator, see Eq. (B1). Thus,  $\mathbf{W}(x)$  must be an odd function and the integral in the numerator of  $\lambda_1$ , being an infinite integral over an odd function, is zero,

$$\lambda_1 = 0, \quad (\text{B9})$$

for all stationary solutions with parity symmetry  $\mathbf{U}_0(x) = \mathbf{U}_0(-x)$ .

- 
- [1] A. Mikhailov and K. Showalter, Phys. Rep. **425**, 79 (2006)
  - [2] *Analysis and control of complex nonlinear processes in physics, chemistry and biology*, edited by Schimansky-Geier, B. Fiedler, J. Kurths, and E. Schöll, Vol. 5 (World Scientific, Singapore, 2007)
  - [3] V. Vanag and I. Epstein, Chaos **18**, 026107 (2008)
  - [4] *Handbook of chaos control*, 2nd ed., edited by E. Schöll and H. G. Schuster (2008)
  - [5] E. Mihaliuk, T. Sakurai, F. Chirila, K. Showalter, *et al.*, Phys. Rev. E **65**, 65602 (2002)
  - [6] J. Schlesner, V. Zykov, H. Engel, and E. Schöll, Phys. Rev. E **74**, 046215 (2006)
  - [7] O. Steinbock, V. Zykov, and S. Müller, Nature **366**, 322 (1993)
  - [8] V. Zykov, O. Steinbock, and S. Müller, Chaos **4**, 509 (1994)
  - [9] J. Schlesner, V. Zykov, H. Brandtstädter, I. Gerdes, and H. Engel, New J. Phys. **10**, 015003 (2008)
  - [10] V. S. Zykov, G. Bordiougov, H. Brandtstädter, I. Gerdes, and H. Engel, Phys. Rev. Lett. **92**, 018304
  - [11] V. Zykov and H. Engel, Physica D **199**, 243 (2004)
  - [12] T. Sakurai, E. Mihaliuk, F. Chirila, and K. Showalter, Science **296**, 2009 (2002)
  - [13] J. Wolff, A. Papathanasiou, H. Rotermund, G. Ertl, X. Li, and I. Kevrekidis, Phys. Rev. Lett. **90**, 018302 (2003)
  - [14] J. Wolff, A. G. Papathanasiou, I. G. Kevrekidis, H. H. Rotermund, and G. Ertl, Science **294**, 134 (2001)
  - [15] J. Wolff, *Lokale Kontrolle der Musterbildung bei der CO-Oxidation auf einer Pt (110)-Oberfläche*, Ph.D. thesis (2002)
  - [16] J. Wolff, A. Papathanasiou, H. Rotermund, G. Ertl, M. Katsoulakis, X. Li, and I. Kevrekidis, Phys. Rev. Lett. **90**, 148301 (2003)
  - [17] P. Kevrekidis, I. Kevrekidis, B. Malomed, H. Nistazakis, and D. Frantzeskakis, Phys. Scr. **69**, 451 (2004)
  - [18] H. Nistazakis, P. Kevrekidis, B. Malomed, D. Frantzeskakis, and A. Bishop, Phys. Rev. E **66**, 015601 (2002)
  - [19] B. Malomed, D. Frantzeskakis, H. Nistazakis, A. Yannacopoulos, and P. Kevrekidis, Phys. Lett. A **295**, 267 (2002)
  - [20] J. Löber and H. Engel [arXiv:1304.2327 \[nlin.PS\]](#)
  - [21] B. Sandstede, Handbook of dynamical systems **2**, 983 (2002)
  - [22] L. Schimansky-Geier, A. S. Mikhailov, and W. Ebeling, Ann. Phys. (Leipzig) **495**, 277 (1983)
  - [23] A. Engel, Phys. Lett. A **113**, 139 (1985)
  - [24] A. Engel and W. Ebeling, Phys. Lett. A **122**, 20 (1987)
  - [25] A. Kulka, M. Bode, and H. Purwins, Phys. Lett. A **203**, 33 (1995)
  - [26] M. Bode, Phys. D **106**, 270 (1997)
  - [27] S. Alonso, J. Löber, M. Bär, and H. Engel, The European Physical Journal Special Topics **187**, 31 (2010)
  - [28] J. Löber, M. Bär, and H. Engel, Phys. Rev. E **86**, 066210 (2012)
  - [29] J. Yan and Y. Tang, Phys. Rev. E **54**, 6816 (1996)
  - [30] J. Yang, *Nonlinear waves in integrable and non-integrable systems* (SIAM, Philadelphia, 2011)
  - [31] A. Pikovsky, M. Rosenblum, and J. Kurths, *Synchronization: a universal concept in nonlinear sciences* (Cambridge University Press, Cambridge, 2003)
  - [32] J. Fröhlich, S. Gustafson, B. L. G. Jonsson, and I. Sigal, Commun. Math. Phys. **250**, 613 (2004)
  - [33] J. Guckenheimer and P. Holmes, *Nonlinear oscillations, dynamical systems, and bifurcations of vector fields* (Springer-Verlag, Berlin, 1983)
  - [34] F. Schlögl, Z. Phys. A **253**, 147 (1972)
  - [35] Y. B. Zel'dovich and D. A. Frank-Kamenetskii, Dokl. Akad. Nauk SSSR **19**, 693 (1938)
  - [36] A. Mikhailov, *Foundations of synergetics I: Distributed active systems* (Springer-Verlag, New York, 1990)

- [37] See Supplemental Material for movies and information on the parameter values chosen for numerical simulations.
- [38] Y. Kuramoto, Prog. Theor. Phys **63**, 1885 (1980)
- [39] Y. Kuramoto, *Chemical oscillations, waves, and turbulence* (Dover, New York, 2003)
- [40] R. FitzHugh, Biophysical J. **1**, 445 (1961)
- [41] J. Nagumo, S. Arimoto, and S. Yoshizawa, Proc. IRE **50**, 2061 (1962)
- [42] J. J. Sakurai, *Modern Quantum Mechanics*, 2nd ed. (Addison-Wesley, MA, 1994)